

# Translational Relaxation of Hot O(<sup>1</sup>D) by Inelastic Collision with N<sub>2</sub> Molecule: Ab Initio MO and Classical Trajectory Studies

Hiroto Tachikawa,<sup>\*,†</sup> Koichi Ohnishi,<sup>‡</sup> Takayuki Hamabayashi,<sup>†</sup> and Hiroshi Yoshida<sup>†</sup>

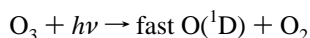
Graduate School of Engineering and Graduate School of Environmental Science, Hokkaido University, Kita-ku, Sapporo 060, Japan

Received: June 14, 1996; In Final Form: November 18, 1996<sup>⊗</sup>

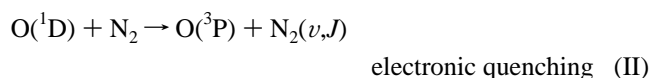
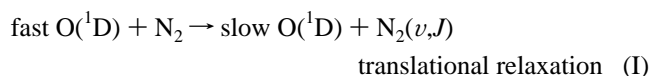
The energy transfer process of translationally hot oxygen atom O(<sup>1</sup>D) by inelastic collision with N<sub>2</sub> molecule, fast O(<sup>1</sup>D) + N<sub>2</sub> → slow O(<sup>1</sup>D) + N<sub>2</sub>(*v*,*J*), has been studied by means of quasi-classical trajectory calculations on the ab initio fitted potential energy surfaces (PESs). The surface hopping procedure was included in the trajectory calculations by the Landau–Zener model in order to consider contribution from the reactive trajectories, i.e., the electronic energy transfer process O(<sup>1</sup>D) + N<sub>2</sub> → O(<sup>3</sup>P) + N<sub>2</sub>(*v*,*J*). Inelastic collisions occurring on <sup>1</sup>A' and/or <sup>3</sup>A' surfaces were only considered in the present study. The results suggest that the cross section for the translational energy transfer process increases with increasing collision energy. Efficiency of the energy transfer from translational to internal modes by a collision was calculated to be 0.45 at a collision energy of 10.0 kcal/mol. The energy relaxation processes of translationally hot O(<sup>1</sup>D) in the upper stratosphere are discussed on the basis of these theoretical results.

## 1. Introduction

The reaction dynamics of the excited oxygen atom O(<sup>1</sup>D), produced in the stratosphere by UV sunlight irradiation, has received much attention from both experimental and theoretical points of view. Primarily, the O(<sup>1</sup>D) atom reacts with several atmospheric molecules and plays an important role in the ozone layer. The singlet oxygen atom, generated by the photodissociation of an ozone molecule



possesses a much larger translational energy and exists as a translationally hot atom.<sup>1</sup> If the atom encounters an N<sub>2</sub> molecule, the energy transfer may occur according to the following two processes:



Process I is a translational-energy transfer from O(<sup>1</sup>D) to the N<sub>2</sub> molecule by collision (i.e., translational relaxation), whereas process II is electronic energy transfer to the N<sub>2</sub> molecule (i.e., an electronic quenching process). Both elastic and inelastic collisions contribute process I. The latter process is caused by the singlet–triplet spin–orbit interaction and involves two potential energy surfaces (singlet/triplet), whereas the former process proceeds on only the singlet surfaces which is composed of five surfaces (<sup>1</sup>Σ, <sup>1</sup>Π, and <sup>1</sup>Δ states in linear form).

Recently we made ab initio MO and surface hopping trajectory calculations to elucidate the detailed reaction dynamics of the electronic-energy transfer process (process II).<sup>2</sup> The results are summarized as follows: (i) the quenching probability decreases with increasing collision energy, and (ii) the electronic

to internal energy transfer occurs efficiently via an intermediate complex N<sub>2</sub>O on singlet surface. The former fact suggests that the process II is favored at low collision energies. Very recently, Matsumi and Chowdhury measured the energy dependence of the cross section of process II by Doppler spectroscopy.<sup>3</sup> They showed that the experimentally observed cross section by the experiment is in excellent agreement with our theoretical values.

Although the translational energy transfer process (process I) brings about the change of internal states of N<sub>2</sub>, the dynamics as inelastic collision is not clearly understood. Studying the energy transfer process of O(<sup>1</sup>D) on the excited state potential energy surface provides important information on the dynamics and mechanism of atmospheric reactions of O(<sup>1</sup>D) atom. In the present study, ab initio MO and quasi-classical trajectory calculations are carried out in order to elucidate the mechanism of energy transfer in inelastic collision of O(<sup>1</sup>D) with N<sub>2</sub>.

## 2. Method of Calculations

In a previous paper,<sup>2</sup> we reported ab initio fitted potential energy surfaces (PESs) for processes I and II on the basis of MP2/6-31G\* calculations. The same potential energy surfaces and the theoretical technique (i.e., surface hopping trajectory calculations) were employed in the present study. The potential energy surfaces obtained shows that the singlet surface is bound by 4.40 eV relative to O(<sup>1</sup>D) + N<sub>2</sub> and the singlet and triplet energy surfaces are crossed at an N–O distance of ca. 1.8 Å.

For linear configuration, there are two triplet states <sup>3</sup>Σ<sup>−</sup> and <sup>3</sup>Π if the N<sub>2</sub>(X<sup>1</sup>Σ<sub>g</sub><sup>+</sup>) and O(<sup>3</sup>P) are brought together. A twofold degeneracy existing for <sup>3</sup>Π splits to <sup>3</sup>A' and <sup>3</sup>A'' in the C<sub>s</sub> point group. Since singlet state X<sup>1</sup>Σ<sup>+</sup> which corresponds to an initial state of O(<sup>1</sup>D) + N<sub>2</sub> reaction becomes <sup>1</sup>A' state in the C<sub>s</sub> point group, <sup>3</sup>A' state will be strongly coupled with <sup>1</sup>A' state. Therefore, we considered the <sup>1</sup>A' and <sup>3</sup>A' PESs for processes I and II. The other singlet surfaces (<sup>1</sup>Δ and <sup>1</sup>Π) are not considered here due to the fact that these surfaces are composed of the strong repulsive shapes. Effects of the contribution from the other surfaces on the dynamics will be discussed in last section on the basis of a preliminary calculation with the <sup>1</sup>Π PES.

The surface hopping probability *P* at each crossing point is calculated on the basis of Landau–Zener model,<sup>4</sup>

<sup>†</sup> Graduate School of Engineering.

<sup>‡</sup> Graduate School of Environmental Science.

<sup>⊗</sup> Abstract published in *Advance ACS Abstracts*, February 1, 1997.

$$P = 1 - P_{\text{LZ}} = 1 - \exp[-2\pi(H_{12})^2/(h\nu|\Delta F|)]$$

where  $\nu$  is the velocity and  $\Delta F$  is a slope difference between potential energy surfaces for the direction perpendicular to the conical intersection seam. The singlet–triplet spin–orbit coupling  $H_{12}$  was assumed to be independent of coordinates and has the value<sup>5</sup>

$$H_{12}(r_1, r_2, \theta) = H_{12} = 80 \text{ cm}^{-1}$$

where  $r_1 = r(\text{O–N})$ ,  $r_2 = r(\text{N–N})$ , and  $\theta$  is O–N–N angle. Note that the trajectory calculations on ab initio fitted PESs employed here have provided detailed information on the reaction dynamics for several reaction systems.<sup>6</sup>

### 3. Results

**A. A Sample Trajectory for Process I.** In order to elucidate characteristics of process I, the potential energy, interatomic distances, and the O–N–N bond angle are calculated for a sample trajectory as a function of reaction time. These values for the sample trajectory with a collision energy of 10.0 kcal/mol are plotted in Figure 1. A trajectory started at time zero, from the distance between the oxygen atom and  $\text{N}_2$  molecule of 6.3 Å, gradually approaches the complex well. A fine structure in the potential energy curve, observed at the range of reaction time 0–0.1 ps, is caused by the N–N stretching mode.

Although the trajectory crossed the seam at a time of 0.15 ps, the surface hopping did not occur because the transition probability calculated by the Landau–Zener model was not satisfied. The trajectory crossed the seam a total of six times, but the hopping did not occur in this trajectory. This trajectory goes back the entrance region again, so that the trajectory become process I.

The lifetime of the  $\text{N}_2\text{O}$  complex for this sample trajectory is estimated to be 0.45 ps, which is smaller than the RRK lifetime (about 3 ps). Therefore, process I does not completely proceed statistically. The corresponding internuclear distances of the sample trajectory are plotted in Figure 1 (middle). It should be noted that the N–N stretching mode is hardly excited at all by this collision. Instead, the rotational mode of  $\text{N}_2$  was excited in the deep potential well as can be seen in Figure 1 (lower).

**B. Rotational and Vibrational State Distributions of the Product  $\text{N}_2(\nu, J)$ .** The rotational state distributions of the  $\text{N}_2(\nu, J)$  molecules produced by process I are summarized in Figure 2. The distributions are close to the Boltzmann one. Peaks of the distributions at  $E_{\text{coll}} = 5, 10, 15$ , and 20 kcal/mol are obtained at  $J = 18, 20, 22$ , and 25, respectively. The peak moves to the higher energy region and the shape becomes broader as the collision energy increases.

Vibrational state distributions calculated as a function of  $E_{\text{coll}}$  are also listed in Table 1. At  $E_{\text{coll}} = 10.0$  kcal/mol, the vibrationally excited state of  $\text{N}_2(\nu = 1)$  is only 1.3% generated. This result suggests that the energy transfer from translational to vibrational modes does not efficiently occur in process I. The energy transfer to rotational modes of  $\text{N}_2$  is dominant.

**C. Summary of the Surface Hopping Trajectory Calculations.** The surface hopping trajectory calculations were performed for up to 16 800 trajectories for each collision energy. As can be clearly seen in Table 1, the probability for process I ( $N_{\text{I}}/N_{\text{total}}$ ) increases with increasing collision energy, where  $N_{\text{total}}$  and  $N_{\text{I}}$  are respectively number of total trajectories and of trajectories for process I. On the other hand, the probability for process II ( $1 - N_{\text{I}}/N_{\text{total}}$ ) decreases as a function of collision

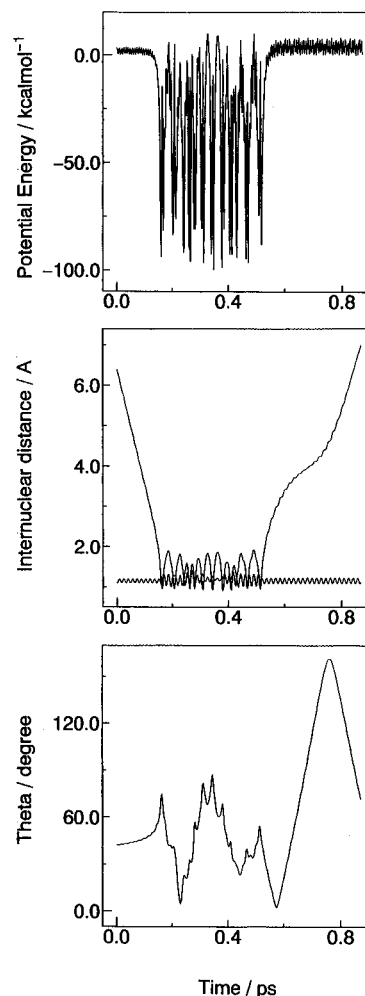


**Figure 1.** Sample trajectory for the inelastic collision, fast  $\text{O}(^1\text{D}) + \text{N}_2 \rightarrow \text{slow O}(^1\text{D}) + \text{N}_2(\nu, J)$ , plotted for the potential energy (upper) and  $r(\text{O–N})$  and  $r(\text{N–N})$  (middle) and angle of O–N–N (lower) versus time. The values are calculated by surface hopping trajectory calculations.

energy. These results suggest that process I proceeds preferentially at high collision energy, while the electronic energy transfer dominates at low-collision energy below 5 kcal/mol.

The averaged internal and kinetic energies of product  $\text{N}_2$  are listed in Table 1. At  $E_{\text{coll}} = 10.0$  kcal/mol, the ratio of the internal energy to the available energy ( $E_{\text{int}}/E_{\text{avail}}$ ) is found to be 0.45, suggesting that the collision causes a slowdown of velocity, namely, lowering of the kinetic energy ( $E_{\text{kin}}$ ) to 7.14 kcal/mol (center-of-mass collision energy).

### 4. Discussion

We discuss the mechanism of the energy transfer process from hot  $\text{O}(^1\text{D})$  to  $\text{N}_2$  molecules. UV photodissociation of ozone at the Hartley bands produces  $\text{O}(^1\text{D})$  and  $\text{O}(^3\text{P})$  with quantum yields of 0.9 and 0.1, respectively.<sup>7</sup> The triplet oxygen formation channel,  $\text{O}_3 \rightarrow \text{O}(^3\text{P}) + \text{O}_2$ , is therefore negligible because of its low yields. This is due to the fact that the excited state of  $\text{O}_3(^1\text{B} \leftarrow ^1\text{A})$  correlates to the  $\text{O}_2(^1\Delta) + \text{O}(^1\text{D})$  state. Valentini et al. measured the fraction of energy disposal to internal energy in the photodissociation of  $\text{O}_3$  at  $\lambda = 240$  nm which is 0.1–0.5 (average = 0.25).<sup>8</sup> By using these data, the translational energy of  $\text{O}(^1\text{D})$  is estimated to be 8–14.5 kcal/mol (average = 12.1 kcal/mol) for the laboratory frame. The center of mass collision energy ( $E_{\text{coll}}$ ) is calculated by

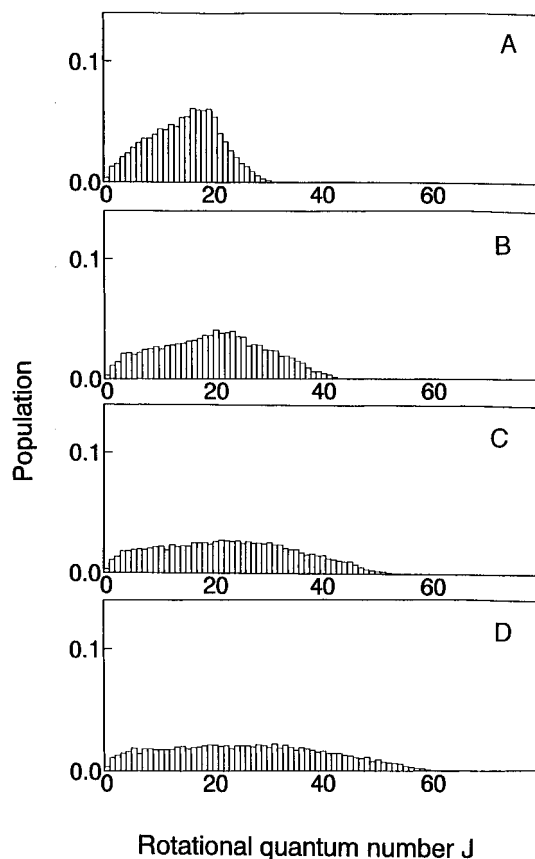


**Figure 2.** Rotational state populations of the  $N_2(v=0)$  molecule formed by the inelastic collision,  $\text{fast O}(^1\text{D}) + N_2 \rightarrow \text{slow O}(^1\text{D}) + N_2(v,J)$ . The collision energies are 5.0 (A), 10.0 (B), 15.0 (C), and 20.0 kcal/mol (D).

**TABLE 1: Summary of the Trajectory Calculations: Probabilities ( $N_i/N_{\text{total}}$ ) of the Translational Energy Transfer Process,  $\text{fast O}(^1\text{D}) + N_2 \rightarrow \text{slow O}(^1\text{D}) + N_2(v,J)$ , Populations of Vibrational Mode of  $N_2(v)$ , and Averaged Internal ( $E_{\text{int}}$ ) and Kinetic ( $E_{\text{kin}}$ ) Energies (kcal/mol)<sup>a</sup>**

$E_{\text{coll}}$	$N_i/N_{\text{total}}^c$	population			averaged energy <sup>b</sup>		
		$v=0$	$v=1$	$v=2$	$E_{\text{int}}$	$E_{\text{kin}}$	$E_{\text{int}}/E_{\text{avail}}$
5.0	0.432	1.000	0.000	0.000	4.06	3.94	0.508
10.0	0.916	0.987	0.013	0.000	5.86	7.14	0.451
15.0	0.949	0.933	0.067	0.001	7.47	10.53	0.415
20.0	0.966	0.885	0.103	0.012	8.39	14.61	0.365

<sup>a</sup> The values are calculated as a function of collision energy  $E_{\text{coll}}$  (in kcal/mol). <sup>b</sup>  $E_{\text{avail}} = E_{\text{coll}} + E_{\text{int}}^0$ , where  $E_{\text{int}}^0$  is internal energy of  $N_2$  for the initial state. <sup>c</sup> Numbers of trajectories formed via process I.

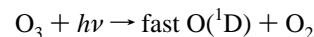
$$E_{\text{coll}} = \frac{1}{2} \frac{m_0 m_{N_2}}{m_0 + m_{N_2}} \left[ \frac{2}{m_0} E_t^{\text{LAB}} + \frac{2}{m_{N_2}} \frac{3}{2} kT \right]$$

for this reaction system, where  $m_i$  is mass of oxygen atom or  $N_2$  molecule,  $k$  Boltzmann constant,  $T$  temperature, and  $E_t^{\text{LAB}}$  translational energy in the laboratory frame. By using this relation,  $E_{\text{coll}}$  is estimated to be 5.4–9.6 kcal/mol (average = 8.0 kcal/mol). This energy suggests that the oxygen atom produced by photodissociation of ozone has a large translational energy.

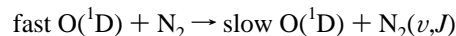
At the collision energy of 10 kcal/mol, the probability for electronic-energy transfer ( $N_{\text{II}}/N_{\text{total}} = 1 - N_{\text{I}}/N_{\text{total}}$ ) is calculated to be 0.084, which is significantly small for a quenching probability. By contrast, the probability for translational-energy transfer is 0.916, suggesting that the translational energy relaxation (process I) is dominant at high collision energies. The collision (process I) causes a slowdown of the kinetic energy

of the excited oxygen atom  $\text{O}(^1\text{D})$ . After several collisions, the electronic-energy transfer process (process II) has proceeded efficiently. In addition to the inelastic collisions, elastic collision (leading to momentum transfer) would occur, so that the velocity of  $\text{O}(^1\text{D})$  is further slowed down.

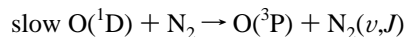
On the basis of our theoretical results, we would like to propose a reaction model for  $\text{O}(^1\text{D})$  in the upper stratosphere. In the first step, the excited oxygen atom  $\text{O}(^1\text{D})$  is generated by the UV photodissociation of  $\text{O}_3$  molecule in upper stratosphere.



Since the oxygen atom  $\text{O}(^1\text{D})$  has a large translational energy, the translational-energy transfer process (process I)



is dominant. This process is composed of both elastic and inelastic collisions. After slowdown by the collision, the electronic-energy transfer



electronic quenching

can occur efficiently. It can be concluded that this energy transfer mechanism is the dominant pathway found in the stratospheric ozone layer.

In the present study, the  $^1\Sigma$  state PES was only considered for the singlet surface because the PES strongly correlates to the quenching process. However, inelastic collision on both  $^1\Delta$  and  $^1\Pi$  state PESs may contribute process I. Hence, a preliminary trajectory calculation on the  $^1\Pi$  state PES ( $^1A'$  state) was performed for comparison. The  $^1\Pi$  state PES was calculated at the singly excited CI level with 6-31G\* basis set, and 1600 trajectories were run for each collision energy. The ratios of ( $E_{\text{int}}/E_{\text{avail}}$ ) at  $E_{\text{coll}} = 5, 10, 15$ , and 20 kcal/mol were calculated to be 0.24, 0.183, 0.151, and 0.133, respectively, suggesting that the efficiency of the energy transfer from translational to internal modes decreases with increasing collision energy as well as  $^1\Sigma$  state PES, although the magnitude is 3 times less than  $^1\Sigma$  state PES. Hence it can be concluded that process I proceeds almost on  $^1\Sigma$  state attractive PES, while the repulsive surfaces slightly contribute the energy loss process.

We considered only inelastic collisions of  $\text{O}(^1\text{D})$  and  $N_2$  in the present study throughout. Elastic collisions would contribute process I as well as the inelastic collisions. The calculation of efficiency for elastic collision<sup>9</sup> may provide overall reaction cross section of  $\text{O}(^1\text{D})$ .

**Acknowledgment.** The authors are indebted to the Computer Center at the Institute for Molecular Science (IMS) for the use of the computing facilities. H.T. acknowledges a partial support from a Grant-in-Aid for Encouragement of Young Scientist from the Ministry of Education, Science and Culture of Japan.

## References and Notes

- (1) (a) For a recent review: Gonzales-Urena, A.; Vetter, R. *J. Chem. Soc., Faraday Trans.* **1995**, *91*, 389, and references therein. (b) Matsumi, Y.; Inagaki, Y.; Morley, G. P.; Kawasaki, M. *J. Chem. Phys.* **1994**, *100*, 315. (c) Abe, M.; Inagaki, Y.; Springsteen, L. L.; Matsumi, Y.; Kawasaki, M.; Tachikawa, H. *J. Phys. Chem.* **1994**, *98*, 12641.
- (2) Tachikawa, H.; Hamabayashi, T.; Yoshida, H. *J. Phys. Chem.* **1995**, *99*, 16630.
- (3) Matsumi, Y.; Chowdhury, A. M. S. *J. Chem. Phys.* **1996**, *104*, 7036.
- (4) (a) Landau, L. D. *Phys. Sov. Union* **1932**, *2*, 46. Zener, C. *Proc. R. Soc. London Ser. A* **1932**, *A137*, 696. (b) Stine, J. R.; Muckerman, J. T. *J. Chem. Phys.* **1976**, *10*, 3975.

- (5) Yamanouchi, T.; Horie, H. *J. Phys. Soc. Jpn.* **1952**, 7, 52.
- (6) (a) Tachikawa, H. *J. Phys. Chem.* **1995**, 99, 225. (b) Tachikawa, H.; Takamura, H.; Yoshida, H. *J. Phys. Chem.* **1994**, 98, 5298. (c) Tachikawa, H.; Tomoda, S. *Chem. Phys.*, **1994**, 182, 185. (d) Tachikawa, H.; Lunell, S.; Tornkvist, C.; Lund, A. *J. Mol. Struct (THEOCHEM)* **1994**, 304, 25. (e) Tachikawa, H.; Ohtake, A.; Yoshida, H. *J. Phys. Chem.* **1993**, 97, 11944. (f) Tachikawa, H.; Hokari, N.; Yoshida, H. *J. Phys. Chem.* **1993**, 97, 10035.
- (7) Wayne, R. P. *Atmos. Environ.* **1987**, 21, 1683.
- (8) Valentini, J. J.; Gerrity, D. P.; Phillips, D. L.; Nieh, J.-C.; Tabor, K. D. *J. Chem. Phys.* **1987**, 86, 6745.
- (9) See for instance: Geiger, L. C.; Schatz, G. C.; Harding, L. B. *Chem. Phys. Lett.* **1985**, 114, 520.